Proceedings of the 3rd ITB Graduate School Conference ISSN: 2963-718X
Enhancing Creativity in Research Through Developing Innovative Capabilities
December 21, 2022

Design and Analysis of 5 MW Kaplan Runner Wheel for Small Hydro Powerplant

Muhammad Febrilian Syah[1,*], Priyono Soetikno[1] & Isnain 'Aliman[2]

[1] Faculty of Mechanical and Aerospace Engineering, Institut Teknologi Bandung
[2]Department of Mechanical Engineering, The University of Melbourne
[*]Email: 23122003@mahasiswa.itb.ac.id

Abstract. In 2019 to 2028, Indonesia will build power plants by utilizing new and renewable energy with 9.5 GW comes from hydro power plants [5]. One of the realizations of the small hydro power plant in Indonesia is a power plant located on the Minahasa Peninsula, North Sulawesi, Indonesia that uses two runners with 5 MW generated from each runner. In this research, the suitable Kaplan runner will be designed complete with the spiral casing, guide vane, and draft tube with a desired capacity of 5 MW and flowrate of 39 m^3/s. The research was started by designing the runner geometry, draft tube, spiral casing, and guide vane and simulated using RANS Computational Fluid Dynamics at steady state in various variation. Variations used in this research are runner blade angle and guide vane angle. The results of the variation of the guide vane angle at each runner blade angle show the increase of hydraulic efficiency until it reaches a certain peak point before decrease. The configuration that produces the highest efficiency at 150 RPM operating rotational speed achieved at -2.5° blade angle and 39.5° guide vane angle with 6.49 MW hydraulic power and 84% efficiency.

Keywords: *computational fluid dynamics; draft tube; guide vane; hydroelectric power plant; kaplan runner; spiral casing.*

Nomenclature

n	=	runner rotational speed (RPM)
P	=	runner hydraulic power (kW)
H	=	head (m)
n_s	=	runner specific speed
N'_{sd}	=	runner power specific speed
D_{tip}	=	runner tip diameter (m)
D_{hub}	=	hub diameter (m)
N	=	hub dan tip diameter ratio
Q	=	flow rate (m^3/s)
ω	=	rotational speed (rad/s)
ε	=	runner glide angle (rad)
g	=	gravitational acceleration (m/s^2)
η_s	=	draft tube efficiency

η_{th} = runner theoretical efficiency
s'' = chord length (m)
t'' = distance between blades (m)
V_1 = inlet water velocity (m/s)
C_{u1} = tangential absolute velocity (m/s)
V_{f1} = meridian absolute velocity (m/s)
U_1 = blade velocity at leading edge (m/s)
U_2 = blade velocity at trailing edge (m/s)
V_{r1} = relative velocity at blade inlet (m/s)
V_{ru1} = tangential relative velocity at blade inlet (m/s)
β_1 = blade inlet angle (^{o})
β_2 = blade outlet angle (^{o})
V_{r2} = relative velocity at blade outlet (m/s)
V_{ru2} = tangential relative velocity at blade outlet (m/s)

1 Introduction

Electrical energy is a basic human need, which continues to increase in direct proportion to the level of welfare. In 2030, Indonesia's population is predicted to reach 296 million people [1]. Population increase is followed by an increase in energy needs, including electrical energy. Indonesia's per capita electricity consumption in 2030 it is expected to reach 3,201 MWh/capita [2]. Therefore, it is necessary to add adequate power plants. Currently, the most widely used power plants are fossil fuel plants including in Indonesia which is dominated by steam power plants with 49.85% [3].

The usage of fossil-based power plant is less profitable considering the limited amount of fossil fuels and the resulting pollution is not good for the environment. For this reason, the community is required to find unlimited and environmentally friendly energy sources called renewable energy. There are several types of renewable energy that can be converted into electrical energy including hydro power [4]. In 2019 to 2028 power plants will be built by utilizing new and renewable energy with a total capacity of up to 16.7 GW. Among the total capacity, 9.5 GW of which comes from hydro and micro hydro power plants [5].

The essential part of converting hydro power into electricity is the runner. There are several types of runners such as Kaplan, Francis, and Pelton. Types of runners have different geometry and best operating conditions based on the net head, flow rate, and specific speed [6]. Table 1 shows the runner type and the suitable operating head range in meters. In addition to the runner, there are several other parts to support the energy conversion system of water flow into electrical energy including spiral casing, guide vane, and draft tube.

Table 1 Head range on each runner type [6]

Runner Type	Head (m)
Kaplan and *Propeller*	2 < H < 40
Francis	10 < H < 350
Pelton	50 < H < 1300
Michell-Banki	3 < H < 250
Turgo	50 < H < 250

Several studies already conducted in small hydropower system design including energy generation potential and component design. Leon *et al.* stated that water use can be optimized if the ratio of the net head does not exceed 15% gross head [7]. In draft tube design, Fulzele *et al.* stated that elbow draft tube type with circular inlet and rectangular outlet has efficiency range from 60% to 80% [8]. In the runner design, Zhang et al proposed series of equation for Kaplan runner. The equation proposed combined the geometric design with the dynamic operation to validate runner design and CFD simulations [9]. Abeykoon *et al.* developed the design and analysis of Kaplan runner wheel for 6 meters head and 5 m3/s flow rate and analyse the design using CFD analysis. According to CFD result, there is significant difference between the theoretical calculation efficiency and the simulation result efficiency where the theoretical efficiency is 94% and the efficiency of the simulation results is 50.98% [10]. Min also developed design for 50 kW Kaplan runner with the different flow condition from research conducted by Abeykoon *et al.* with the runner design result have different operating condition especially in guide vane opening angle and blade angel to achieve desired power shaft output [11]. The runner design may be varied due to the different flow characteristic between one region and another therefore runner design must be proposed for certain power output, head, and flowrate according to the potential that exists in the runner installation area.

One of the realizations of the small hydro power plant in Indonesia is a power plant located on the Minahasa Peninsula, North Sulawesi, Indonesia. The total power generated is 9.9 MW uses two runners with 5 MW generated from each runner. Water discharge for one runner is 39 m^3/s. The water reservoir used on the runner comes from dam located on the Bone River, North Sulawesi. The water level in the dam has a range of 94 to 96 meters above sea level with the runner installation system placed at a height of 78 meters above sea level and the minimum tail race water level is almost parallel to the runner installation height. According to the water level at the dam and tailrace, the head obtained is at a low head with the suitable runner type is the Kaplan runner.

In this study, a Kaplan runner was designed complete with a spiral casing and a draft tube with a capacity of 5 MW and a flow rate of 39 m^3/s with various variations, such as varying the angle of the guide vane and varying the angle of the runner. The variation intended to obtain the performance characteristic in the water runner in form of power and efficiency. The results of the design through analytical methods will be validated using Computational Fluid Dynamics (CFD)-based software, namely RANS Computational Fluid Dynamics.

2 Methods

The method used in this study begins by determining runner parameter from the given case study and continues with the design of the runner. The runner design process begins with developing the runner design continued with designing the guide vane, spiral casing, and draft tube. After all components have been designed, assembly is carried out using the design components to be simulated in RANS Computational Fluid Dynamics to obtain the characteristics and performance of the designed water turbine.

2.1 Runner Design

The operating conditions on the turbine are used to calculate runner specific speed. The operating parameter for runner is shown in Table 2. The value of the specific speed as a function of power (n_s) and power specific speed can be calculated using Eq. (1) and Eq. (2). With n is rotational speed, P is hydraulic power, and H is net head.

$$n_s = n\frac{\sqrt{P}}{H^{5/4}} \tag{1}$$

$$N'_{sd} = \frac{n\sqrt{1.341P}}{[3.28H]^{5/4}} \tag{2}$$

Table 2 Operating Parameter for Runner

Parameter	Value	Unit
Hydraulic power (P)	5	MW
Rotational speed design	200	RPM
Rotational speed operation	150	RPM
Net head (H)	14.5	Meters
Water Flowrate	39	m^3/s

The draft tube that will be used is elbow type with circular inlet and rectangular outlet. The efficiency of the draft tube with this type is in the range of 60% to 80% [8]. In this study, the draft tube is assumed to have an efficiency of 67.5%. The airfoil used is NACA 6409 with angle of attack 5°. The diameter of the runner will be determined using Eq. (3) and Eq. (4) [12]. N is the ratio of D_{tip} and D_{hub} with the value of 0.4 and number of blades 5 [12], Q is the flowrate, ω is rotational speed in rad/s, g is gravity acceleration, η_s is draft tube efficiency, and ε is the glide angle in rad.

$$D_{tip} = 1{,}155 \left(\frac{1-\eta_s}{K_o \omega \varepsilon g H}\right)^{\frac{1}{7}} \left(\frac{Q}{1-N^2}\right)^{\frac{3}{7}} \quad (3)$$

$$K_o = \frac{2}{3} \times \frac{(1-N^2)}{(1-N^3)} \quad (4)$$

The velocity triangle will be used to determine the shape of the blade theoretically. A velocity triangle review is carried out on a cross section of the blades in five different radial distances measured from the centre of the hub. The five distances will be named R1, R2, R3, R4, and R5 with equation Eq. (5). The velocity triangle in the cross section of the blade can be seen in Figure 1. Further calculations for each parameter in velocity triangle will be carried out using Eq. (6) until Eq. (14) where i are 1,2,3,4, and 5 [14]. The relative velocity of the tangential direction, relative velocity, and angle to the horizontal at the centre of the blade will be determined using Eq. (15) until Eq. (17) [10]. From the equation, the subscript 1 is indicated the value of respective variable at the inlet and subscript 2 is at the outlet. V and U is water velocity and blade velocity due to rotation. C_u and V_f is tangential and meridian absolute velocity. V_r and V_{ru} is relative and tangential relative velocity. β is the blade angle and α is the angle between inlet water velocity and blade velocity due to rotation.

The ratio between the chord length and the distance between the blades will be set to 0.75 for the hub diameter section and 1.3 for the tip diameter section [10]. The distribution of the value of s"/t" and the value of t" is based on Eq. (18) and Eq. (19) with s" is the chord length and t" is the distance between blades. The value of β_1 must first be adjusted to the optimal blade angle that has been determined previously for the NACA 6409 airfoil, which is 5°. After adjusting to the 5° blade angle, then the $\beta_{rotation}$ will be defined which is the rotation value in the form of twist angle that must be given to the NACA 6409 airfoil profile. $\beta_{rotation}$ will be calculated based on Eq. (20).

$$R_i = \frac{D_{hub}}{2} + \frac{i-1}{4}\left(\frac{D_{tip}-D_{hub}}{2}\right) \quad (5)$$

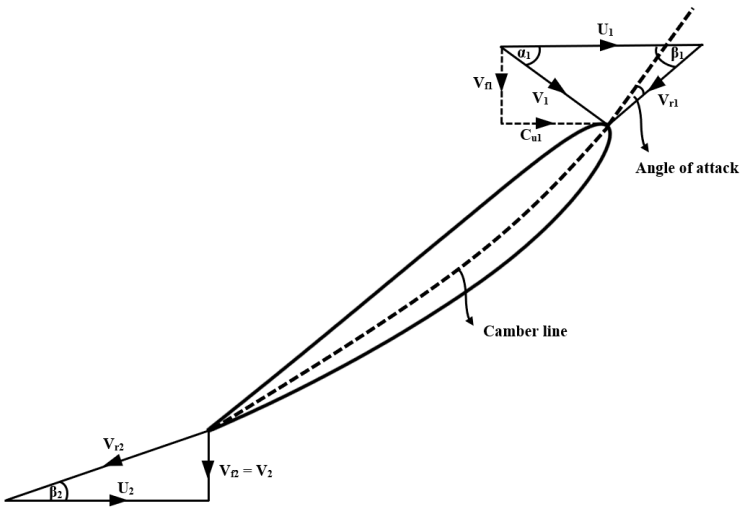

Figure 1 Cross section of blade and speed triangle [13]

$$v_{f1} = \frac{Q}{\frac{\pi}{4}(D_{tip}{}^2 - D_{hub}^2)} \tag{6}$$

$$U_1(i) = U_2(i) = \frac{2\pi R_i n}{60} \tag{7}$$

$$C_{u1}(i) = \frac{\eta_{th} g H}{U_1(i)} \tag{8}$$

$$\tan\beta_1(i) = \frac{v_{f1}}{U_1(i) - C_{u1}(i)} \tag{9}$$

$$\tan\beta_2(i) = \frac{v_{f2}}{U_2(i)} = \frac{v_{f1}}{U_1(i)} \tag{10}$$

$$v_{r1}(i) = \sqrt{v_{f1}^2 + (U_1(i) - C_{u1}(i))^2} \tag{11}$$

$$v_{r2}(i) = \sqrt{v_{f2}^2 + (U_2(i))^2} \tag{12}$$

$$\alpha(i) = tan^{-1}\left(\frac{v_{f1}}{C_{u1}(i)}\right) \tag{13}$$

$$C_{u\infty}(i) = \frac{C_{u1}(i)}{2} \tag{14}$$

$$v_{ru\infty}(i) = U_1(i) - C_{u\infty}(i) \tag{15}$$

$$v_{r\infty}(i) = \sqrt{(v_{ru\infty}(i))^2 + v_{f1}{}^2} \tag{16}$$

$$\beta_\infty(i) = tan^{-1}\left(\frac{v_{f1}}{v_{ru\infty}}\right) \tag{17}$$

$$\left(\frac{s"}{t"}\right)_i = 0.75 + 0.55\left(\frac{i-1}{4}\right) \tag{18}$$

$$t"(i) = \frac{2R_i\pi}{Number\ of\ Blades} \tag{19}$$

$$\beta_{rotation}(i) = 180^0 - \beta_1(i) + 5^o \quad (20)$$

2.2 Guide vane, spiral casing, and draft tube design

NACA 2.5411 airfoil type is selected for guide vane profile. Several parameters will be assumed for the guide vane design including the chord length (L) 0.75 meters, guide vane height (H) 1 meter, the outer diameter (D_{gv}) of the guide vane circuit is 3.92 meters, and the number of guide vanes is 16.

Spiral casing is the component that provide uniform flow to the guide vane with cross-sectional area of the flow should decrease gradually along the circumference of the spiral casing [15]. The dimensions used in the design of the spiral casing are based on Figure 2. Furthermore, the cross-section of the flow area used is based on the places of runner is coincidence with the spiral casing according to Figure 2. The shape of the draft tube with elbow type can be seen in Figure 3 with the dimension for the draft tube are calculated using Eq. (21) until Eq. (30) with D_{tip} is the tip diameter and n_s is the specific speed.

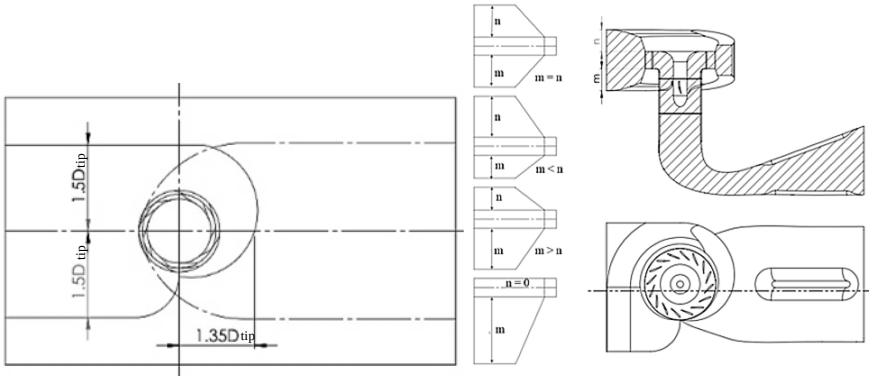

Figure 2 Spiral Casing Dimension (left) and Cross-sectional area of flow in Spiral casing (right) [15]

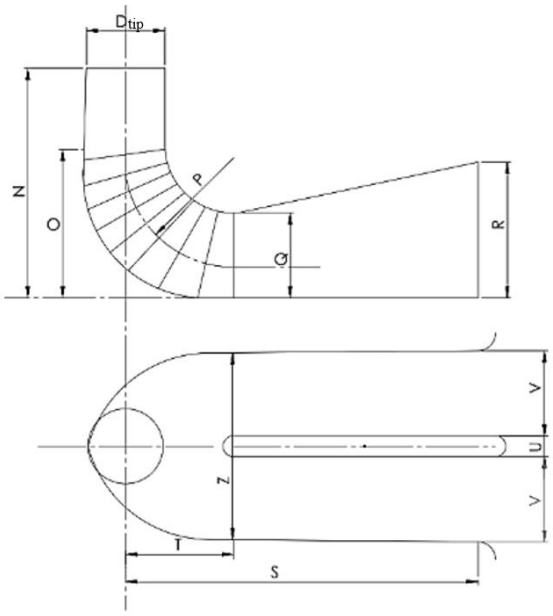

Figure 3 Elbow Type Draft Tube [15]

$$N = D_{tip}\left(1{,}54 + \frac{203{,}5}{n_s}\right) \quad (21)$$

$$O = D_{tip}\left(0{,}83 + \frac{140{,}7}{n_s}\right) \quad (22)$$

$$P = D_{tip}(1{,}37 - 0{,}00056n_s) \quad (23)$$

$$Q = D_{tip}\left(0{,}58 + \frac{22{,}6}{n_s}\right) \quad (24)$$

$$R = D_{tip}\left(1{,}6 - \frac{0{,}0013}{n_s}\right) \quad (25)$$

$$S = \frac{D_{tip}n_s}{(-9{,}2+0{,}25n_s)} \quad (26)$$

$$T = D_{tip}(1{,}5 + 0{,}00019n_s) \quad (27)$$

$$U = D_{tip}(0{,}51 - 0{,}0007n_s) \quad (28)$$

$$V = D_{tip}\left(1{,}1 + \frac{53{,}7}{n_s}\right) \quad (29)$$

$$Z = D_{tip}\left(2{,}63 + \frac{33{,}8}{n_s}\right) \quad (30)$$

2.3 Numerical Simulation

The numerical simulation process is carried out using the RANS Computational Fluid Dynamics software. The simulation used is steady state single phase simulation with k-ω SST turbulence model. k-ω SST has the advantage of predicting flow near the wall and away from the wall [16].

The spiral casing, guide vane, and draft tube components will be given a water-liquid type of fluid without any frame motion. The runner component will be given a water-liquid type of fluid with a frame motion in the form of rotation on the y-axis with a rotational speed of 150 RPM. Runner blade and runner hub wall condition converted into a moving wall in the form of rotation with a rotational speed of 0 RPM relative to the appropriate cell condition and the axis of rotation is on the y-axis.

At the outlet and inlet, the boundary conditions used are pressure outlet and inlet. The inlet pressure is determined by hydrostatic pressure according to net head. Turbo topology in RANS Computational Fluid Dynamics is defined to determine the topology of turbo engine applications so that the special post processing features of turbo topology can be used to see the performance of the designed runner.

2.4 Mesh independency test

Mesh independence test aims to determine the smallest number of meshes needed to ensure that the simulation shows results that are not much different when the number of meshes is varied. The parameter that will be seen in the mesh independence test is the average mass flow rate at the inlet and outlet with the error will be determined by (31). The smallest number of meshes that show mass flow rate errors less than 1% will be used in the simulation.

$$\%Error = \left| \frac{\dot{m}_{avg}^{previous} - \dot{m}_{avg}^{current}}{\dot{m}_{avg}^{current}} \right| \times 100\% \qquad (31)$$

3 Results and Discussions

The result of design feature calculation according to the case study given in Table 2 are shown in Table 3. Data from Table 3 is used for calculation using Eq. (5) until Eq. (20) to obtain the theoretical calculation parameters of the blade. The calculation result for blade theoretical parameters is shown in Table 4. The data from Table 4 will be used to determine the runner airfoil coordinates in each segment. The result of the component assembly is shown in Figure 4.

Table 3 Design Feature Calculation

Parameter	Value	Unit
n_s design	500	-
n_s operation	375	
N'_{sd} design	130	-
N'_{sd} operation	98	
Efficiency [17]	95	%
Number of blades	6	-
N	0.45	-
Ko	0.58766	-
D	2.53	m

Table 4 Theoretical Calculation Parameters of Blade

Parameter	R1	R2	R3	R4	R5
D (m)	1,14	1,49	1,83	2,18	2,53
R (m)	0,57	0,74	0,92	1,09	1,26
V_{f1} (m/s)	12,08	12,08	12,08	12,08	12,08
U (m/s)	11,94	15,58	19,23	22,87	26,51
C_{u1} (m/s)	11,31	8,67	7,03	5,91	5,10
$C_{u\infty}$ (m/s)	5,66	4,33	3,51	2,95	2,55
α (º)	46,88	54,34	59,81	63,94	67,12
β_1 (º)	87,01	60,22	44,73	35,47	29,44
β_2 (º)	45,33	37,79	32,15	27,85	24,51
β_∞ (º)	62,51	47,05	37,56	31,25	26,76
s"/t"	1,30	1,16	1,02	0,89	0,75
t" (m)	0,59	0,78	0,96	1,14	1,32
s" (m)	0,78	0,90	0,98	1,01	0,99
$\beta_{rotation}$ (º)	97,98	124,78	140,27	149,53	155,56

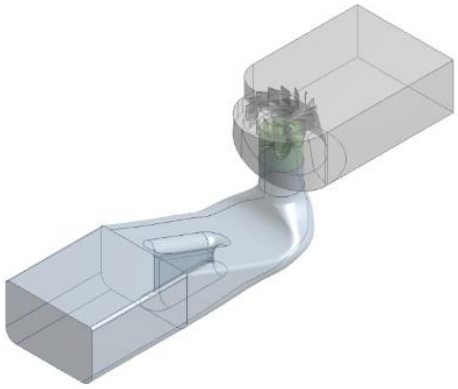

Figure 4 Components Assembly

The value of the mesh used for mesh independency test started from 700 thousand mesh to 2.9 million mesh. The results of the mesh independence test in Figure 5 shows that the number of meshes with the error value of the mass flow rate below 1% starts at 1.7 million meshes so that the number of meshes used as a reference for the simulation is 1.7 million.

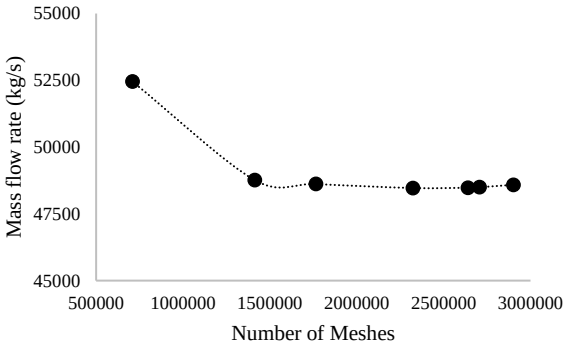

Figure 5 Mesh Independency Test

The variations of the guide vane angle show a tendency to decrease the mass flow rate when the guide vane angle is increased. The decreased mass flowrate is in accordance with the condition of the guide vane which shows that the larger the angle of the guide vane, the smaller the area around the guide vane that may pass the water, so that the mass flow rate will decrease as shown in Figure 6.

Runner hydraulic power at a certain guide vane angle in various variations of runner blade angle can be seen in Figure 7. For each variation of the blade angle, increasing the angle of the guide vane will cause the runner hydraulic power to

increase until it reaches a certain peak before finally decreasing. The simulation results show that the smaller the value of the runner blade angle, the greater the hydraulic power. This increasing hydraulic power is accompanied by a decrease in the operating range of the guide vane angle that can be given. In this study, the target output hydraulic power of 5 MW can be achieved for every blade angle variation.

At each varying blade angle, the value of efficiency will increase as the angle of the guide vane increases as shown in Figure 8. This increase in efficiency lasts until it reaches a certain peak before finally decreasing. The highest efficiency of 84% is obtained from the operating conditions of the guide vane angle of 39.5° and blade angle of -2.5°. The simulation conditions with the closest results to the runner design parameters with a flow rate of 39 m^3/s and a power of 5 MW were obtained with a blade angle configuration of 5° with a guide vane angle of 44.5°

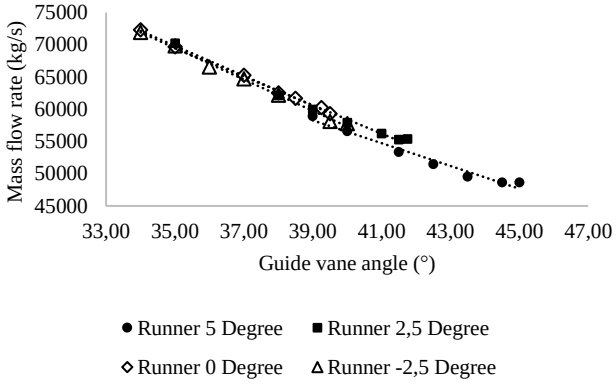

Figure 6 Mass flow rate calculated due to guide vane angle

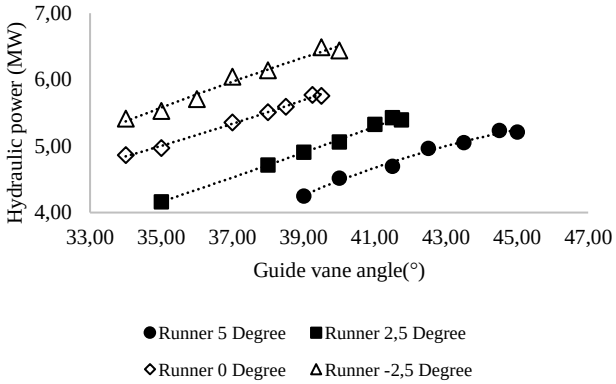

Figure 7 Runner hydraulic power

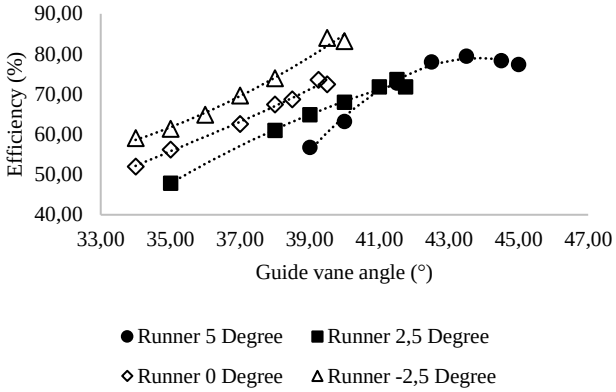

Figure 8 Efficiency versus guide vane angle

The pressure contour and wall shear contour on the blade is shown in Figure 9. Pressure contour indicates that there is cavitation that occurs in the area near the leading edge of the blade. The emergence of cavitation in the simulation results occurs because the conditions of the simulation settings at the outlet are assumed to be at atmospheric pressure while in operating conditions the Kaplan runner generally has an outlet channel below the tailrace water level. The wall shear contour shows that there are several region that have quite small wall shear values on the suction side of the blade. Evaluation of the velocity contour on the Figure 10 shows that in the area on the suction side of the blade, there are region where the velocity has decreased drastically while outside the area, the velocity value is relatively high indicated by the orange color on the contour. The velocity contour indicates that there is a flow separation caused by the non-adjusted thickness of the airfoil in the segment near the runner tip.

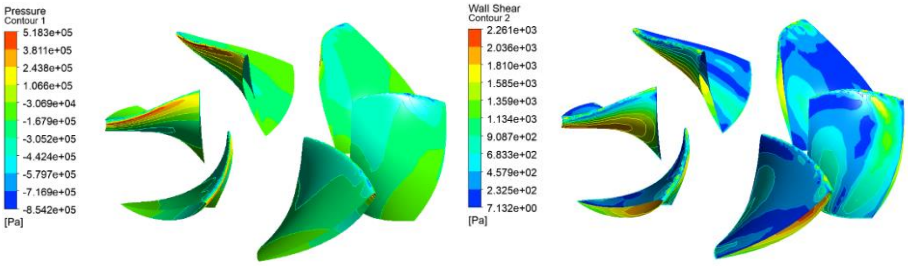

Figure 9 Pressure contour on the runner blade (left) and wall shear contour on the runner blade (right)

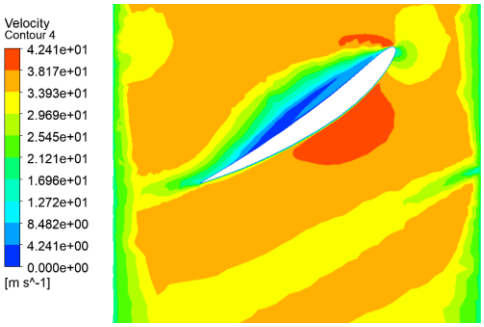

Figure 10 Velocity contour on the blade

4 Conclusions

The designed Kaplan runner has an outer diameter of 2.53 meters and a hub diameter of 1.14 meters with the number of runner blades used is 6 blades with the airfoil profile used is NACA 6409. The number of guide vane blades used is 16 blades with a chord length of 0.75 meters and a height of 1 meter and uses a NACA 2.5411 airfoil. The spiral casing design has a semi-spiral type and the type of draft tube used is elbow type. Target output hydraulic power of 5 MW can be achieved for every blade angle variation. The cavitation may occur at the suction side's leading edge of the blade due to flow separation therefore design optimization may conduct to minimalize the cavitation potential at the runner.

References

[1] Badan Pusat Statistik, "Berita Resmi Statistik No. 7/01/Th.XXIV," no. 27, pp. 1–52, 2021, [Online]. Available: https://papua.bps.go.id/pressrelease/2018/05/07/336/indeks-pembangunan-manusia-provinsi-papua-tahun-2017.html.

[2] Direktorat Jenderal Ketenagalistrikan, "Statistik Ketenagalistrikan 2019," vol. 33, no. 9, pp. 1689–1699, 2020.

[3] Direktorat Jenderal Keteragalistrikan, "Statistik Kelistrikan 2020," Kementrian Energi dan Sumber Daya Miner. Direktrat Jenderal Keteragalistrikan, vol. 13, no. April, p. 122, 2021.

[4] N. Alrikabi, "Renewable Energy Types," J. Clean Energy Technol., no. January 2014, pp. 61–64, 2014, doi: 10.7763/jocet.2014.v2.92.

[5] PT. PLN (Persero), "Electric Power Supply Business Plan (2019-2028)," pp. 2019–2028, 2019, [Online]. Available: http://gatrik.esdm.go.id/assets/uploads/download_index/files/5b16d-kepmen-esdm-no.-39-k-20-mem-2019-tentang-pengesahan-ruptl-pt-pln-2019-2028.pdf.

[6] European Small Hydropower Association, Layman's Guidebook on how to develop a small hydro site. Brussels: Directorate General for Energy, 1998.
[7] A. S. Leon, "A dimensional analysis for determining optimal discharge and penstock diameter in impulse and reaction water turbines," no. August, 2018, doi: 10.1016/j.renene.2014.06.024.
[8] C. D. Fulzele, "Introduction and Design of Elbow Type Draft Tube with Hexagonal Shape at Outlet," vol. 3, no. 1, pp. 1–3, 2020, doi: 10.5281/zenodo.3859299.
[9] Z. Zhang, "Master equation, design equations and runaway speed of the Kaplan turbine," J. Hydrodyn., vol. 33, no. 2, pp. 282–300, 2021, doi: 10.1007/s42241-021-0020-1.
[10] C. Abeykoon and T. Hantsch, "Design and analysis of a Kaplan turbine runner wheel," Proc. World Congr. Mech. Chem. Mater. Eng., vol. 2011, pp. 1–16, 2017, doi: 10.11159/htff17.151.
[11] M. M. Oo, "Design of 50 kW Kaplan Turbine for Micro hydro Power Plant," vol. 3, no. 2, pp. 264–270, 2019, [Online]. Available: http://www.irejournals.com/formatedpaper/1701517.pdf.
[12] J. Raabe, Hydro Power : The Design, Use, and Function of Hydromechanical, Hydraulic, and Electrical Equipment. Dusseldorf: VDI Verlag, 1985.
[13] Z. M. Chan and Z. N. Aung, "Design calculation of Kaplan Turbine Runner Blade for 15kw Micro Hydropower Plant," vol. 5, no. 4, pp. 14–16, 2020.
[14] S. Le Minn, H. H. Win, and M. Thien, "Design and Vibration Characteristic Analysis of 10kW Kaplan Turbine Runner Blade Profile," Int. J. Sci. Eng. Technol. Res., vol. 03, no. 06, pp. 1038–1044, 2014.
[15] R. S. Varshney, Hydro Power Structures (Including Canal Structures and Small Hydro). Roorkee: Nem Chand & Bros, 2001.
[16] D. Adanta, I. M. R. Fattah, and N. M. Muhammad, "COMPARISON OF STANDARD k-epsilon AND SST k-omega TURBULENCE MODEL FOR BREASTSHOT WATERWHEEL SIMULATION," J. Mech. Sci. Eng., vol. 7, no. 2, pp. 039–044, 2020, doi: 10.36706/jmse.v7i2.44.
[17] P. M. Gerhart, A. L. Gerhart, and J. I. Hochstein, Munson, Young, and Okiishi's Fundamentals of Fluid Mechanics, 8th ed. USA: John Wiley & Sons, Inc., 2016.